



ELSEVIER

Journal of Alloys and Compounds 323–324 (2001) 404–407

Journal of
ALLOYS
AND COMPOUNDS

www.elsevier.com/locate/jallcom

Reverse Monte Carlo study of local structural and magnetic cross-correlations in $x = 1/3$ (La,Ca) manganites

F.J. Mompean^{a,*}, A. Møllergård^b, M. García-Hernández^a, D. Sánchez-Soria^a, A. de Andrés^a,
R.L. McGreevy^b, J.L. Martínez^a

^aICMM, CSIC, ES-28049 Madrid, Spain

^bNFL Studsvik, Uppsala University, S-61182 Nyköping, Sweden

Abstract

Local deviations from the average magnetic and atomic structure of $\text{La}_{0.67}\text{Ca}_{0.33}\text{MnO}_3$ are explored by combining neutron diffraction and reverse Monte Carlo techniques. Short range FM Mn–Mn spin pair correlations are found to be a majority well above T_c , while AF correlations between first neighbour pairs of Mn ions develop preferentially around T_c and within those pairs with a distance larger than the average first neighbour Mn–Mn distance. These results agree with the predictions of current theories on phase transitions in double exchange systems. © 2001 Elsevier Science B.V. All rights reserved.

Keywords: Magnetically ordered materials; Chemical synthesis; Exchange and superexchange

1. Introduction

The current search for materials potentially useful for applications in the field of magnetoelectronics has brought about a renewed interest in the study of La-doped manganites with the general formula $\text{La}_{1-x}\text{A}_x\text{MnO}_3$, where A is an alkaline earth cation. These compounds present an intricate phase diagram showing, depending upon the level of doping, a broad phenomenology ranging from ferromagnetic to antiferromagnetic correlations, from metallic or semiconductor behaviour to charge ordered insulators [1].

In particular, $\text{La}_{0.67}\text{Ca}_{0.33}\text{MnO}_3$ shows a paramagnetic to ferromagnetic transition at $T_c = 260$ K, about the same temperature where the electronic transport undergoes a transition from a semiconductor to a metallic regime. Recently, the magnetic transition in $\text{La}_{0.67}\text{Ca}_{0.33}\text{MnO}_3$ was demonstrated to be a first-order transition [2], in contrast to the second-order transition observed for the Sr compound. The electronic transport properties for doping levels $0.15 < x < 0.5$ have been explained in terms of the double exchange mechanism described by Zener [3,4]. Consequently, these systems exhibit intrinsic magnetoresistance (MR) and, in polycrystalline form, have been shown to

also have large extrinsic low field MR effects, related to the existence of grain boundaries [5]. However, the electronic transport properties do not depend solely on the Mn^{4+} doping level and other factor may play a role. For instance, $\text{La}_{0.67}\text{Ca}_{0.33}\text{MnO}_3$ shows a metal–insulator transition around T_c , while $\text{La}_{0.67}\text{Sr}_{0.33}\text{MnO}_3$ remains metallic well above T_c . The observed differences can be understood in light of the current theoretical predictions [6] for the generic phase diagram of these materials. According to these predictions and for these particular levels of doping, the existence of significant antiferromagnetic (AFM) coupling for those compounds showing first-order magnetic transitions and lower T_c seems to be in order, while AFM interactions are negligible for those materials presenting a continuous transition and higher T_c .

In this paper, we address experimentally the search for the postulated short range AFM interactions in $\text{La}_{0.67}\text{Ca}_{0.33}\text{MnO}_3$ on a microscopic scale by probing the atomic and spin correlations with thermal neutron diffraction experiments above and below T_c . We applied reverse Monte Carlo (RMC) analysis of the Bragg and diffuse intensities. In RMC simulations, the atomic and spin coordinates for a set of ions arranged non-periodically within a simulation box are varied at random without any intervening potential. An optimal configuration is found, the calculated powder structure factor of which fits that

*Corresponding author. Fax: +34-91-372-0623.

E-mail address: mompean@icmm.csic.es (F.J. Mompean).

observed. Searches through the optimal configuration for local correlations between structural and magnetic deviations from the average behaviour are then possible.

2. Experiment and data analysis

$\text{La}_{0.67}\text{Ca}_{0.33}\text{MnO}_3$ powder was prepared by the sol-gel technique [7]. Neutron powder diffraction data were collected using the high dynamic range SLAD diffractometer at the NFL reactor in Studsvik (Sweden) for $\text{La}_{0.67}\text{Ca}_{0.33}\text{MnO}_3$ in the temperature range $15 \text{ K} < T < 325 \text{ K}$. The incident energy of the neutrons was $E_i = 67 \text{ meV}$ and $S(Q, w)$ was integrated for $S(Q)$ for all scattering angles in the region $5^\circ < 2\theta < 120^\circ$, resulting in a momentum transfer Q range of $1 < Q(\text{\AA}^{-1}) < 10$; small inelastic contributions to the diffracted intensity in this region might stem from a few phonon branches and low-energy spin waves occurring in the few meV range [8]. Spin diffusion takes place at lower Q values with meV characteristic widths. Careful measurement of the empty container, background and proper subtraction of the contributions due to the empty container, background and multiple scattering were performed. Rietveld refinements of the lattice constants were carried out for a $Pnma$ cell at all measured temperatures.

We attempt to go beyond Rietveld analysis by using a data analysis technique which is not constrained to a single cell description. An immediate consequence of such an approach is the feasibility of accounting for some sort of local disorder and, therefore, the assumption of the probable existence of short range correlations (either magnetic or atomic). This is because, in RMC, the positions of the atoms contained in a simulation box are changed randomly and the new positions are accepted if $S(Q)$ computed from the resulting configuration approaches the experimental values in a least squares sense. In particular, we used a simulation box equivalent to $6 \times 4 \times 6$ $Pnma$ single cells for which the La and Ca atoms are treated as weighted average atoms. Parallel to this structural simulation, classical spins are attached to the positions occupied by magnetic ions, the orientation of which is also changed randomly. The magnetic scattering contribution from this 'magnetic' simulation box is evaluated and added to the structural one in order to make a comparison with the measured structure factor. In our case, only Mn ions carry classical unit spins and the form factor corresponds to a weighted $\text{Mn}^{3+}/\text{Mn}^{4+}$ average. That is, RMC computed scattering accounts for nuclear and magnetic, Bragg and diffuse scattering. The main advantage of our approach is that it provides the atomic and individual localised spin orientations defining the optimal configurations so various correlations can be searched for. For each temperature, all structural and magnetic cells are dressed with atoms and spins as obtained from Rietveld refinement of the experimental data. Minimum interatomic distances and total

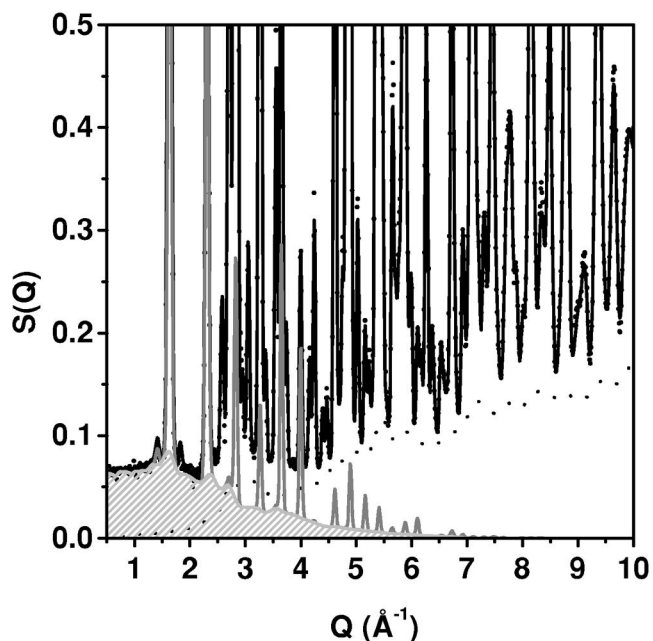


Fig. 1. Neutron diffractogram at $T = 15 \text{ K}$. Dots are experimental data, the dashed line is the structural diffuse scattering, the gray line is the total magnetic contribution, the marked area under the gray line is the magnetic diffuse scattering and the continuous black line is the sum of the former contributions plus the nuclear Bragg scattering.

magnetic moment constraints are applied. Our code RMCPOW [9] also provides for adequate polycrystalline averaging. Fig. 1 shows a representative diffractogram along with the corresponding RMC fit comprising all different contributions to the scattering.

3. Results

We computed the pair correlation function (PCF) for the optimal RMC configurations for both Mn–Mn and Mn–O pairs in the (ac) -plane and along the long axis. These planes and directions are treated as volumes in the 3-D configuration space. Fig. 2a shows the PCF for Mn–Mn at different temperatures. Fig. 2b shows the normalized contributions of the in-plane (a,c) and out-of-plane Mn–Mn to PCF of Mn–Mn. It can be seen that nearest neighbours (NN) along different directions exhibit distance distributions centred around the same values (in accordance with the Rietveld averages). However, the atom pairs in the (a,c) plane seem to account for the tails of the NN distance contributions, while pairs of atoms along the long axis have a narrower distribution. It must, therefore, be underlined that not only do distortions with respect to the averaged structure exist, but these are basically located within the (a,c) plane. This does not support the existence of a breathing mode of the MnO_6 octahedron as claimed by Billinge et al. [10].

Similarly, by evaluating the magnetic moment PCF,

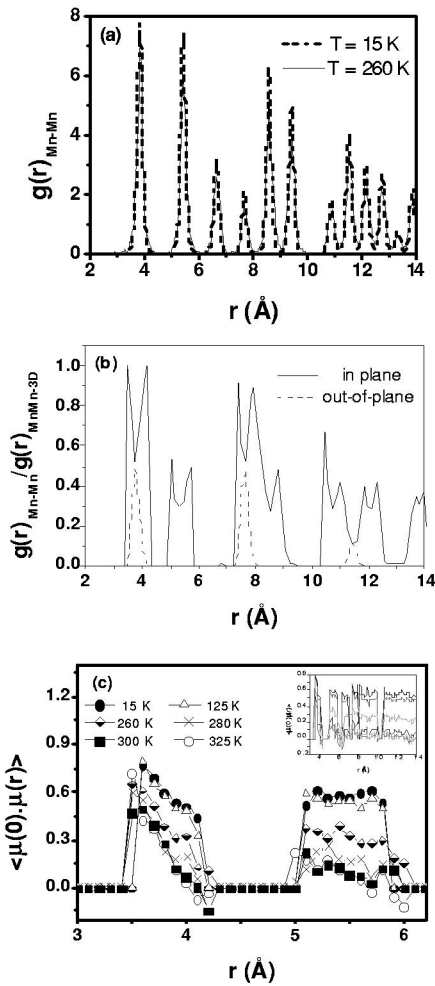


Fig. 2. (a) PCF for Mn–Mn at different temperatures. (b) Normalized contribution to PCF of the ac in-plane and out-of-plane Mn–Mn pairs. (c) Magnetic moment pair correlation function for Mn–Mn pairs.

$\langle \mu(0) \cdot \mu(r) \rangle$, we found that there is a strong change in the average character of the short-range magnetic interactions between the nearest neighbour (NN) ions through T_c . We now focus on the NN correlations in Fig. 2c, since it is mostly for these that we have enough pairs to compute quantities that are definitely sound on a statistical basis. From this figure it is already apparent that for NN Mn–Mn pairs at the shorter distances, the pair magnetic correlations seem to remain FM even above T_c . Certainly, the correlations become short ranged at the highest temperatures. Surprisingly enough, this does not hold for those Mn–Mn pairs at the larger distances, for which $\langle \mu(0) \cdot \mu(r) \rangle$ becomes negative around T_c . This, therefore, suggests the existence of magnetic correlations of an AFM character in these materials. Further, from the structural insight gained with the RMC, we can establish that, on average, these pairs are located in the ac plane (see Fig. 2b), while those pairs at a distance closer to the average structure (Rietveld value) are along the b -axis. Notice also that the loss of FM correlation at low temperature and the growth of a negative

lobule in $\langle \mu(0) \cdot \mu(r) \rangle$ shows a maximum near 280 K and, therefore, some sort of critical behaviour can be conjectured. This behaviour of the negative lobule versus temperature to a great extent rules out systematic numerical errors or spurious experimentally detected signals as the origin of the observed short range AFM correlations. For comparison, the corresponding $\langle \mu(0) \cdot \mu(r) \rangle$ for the twin compound $\text{La}_{0.67}\text{Sr}_{0.33}\text{MnO}_3$ can be found in Ref. [11], where it becomes apparent that a strong decay of the FM correlations develops with increasing temperature, but no hint of AFM short range correlations was reported. From Fig. 3 it can be inferred that the behaviour versus temperature of the negative lobule is lacking in the temperature dependence of the lattice constant and also mostly in the parameter defining the orthorhombic in-plane distortion of the octahedra, $2(a-c)/(a+c)$, as derived from the Rietveld fittings. However, it correlates with the equivalent local quantity $[2\text{MnO}(2) - \text{MnO}(1)]/[\text{MnO}(2) + \text{MnO}(1)]$ calculated from the PDF Mn–O of the RMC configurations. As a general trend it is also observed that the angle Mn–O–Mn for those manganese atoms with AFM interactions shows a distribution slightly displaced towards larger values. Similarly, these atoms are located at larger distances of the intermediate oxygen than its FM counterpart. This increase could explain the AFM character of the interactions since the larger the Mn–O distance the smaller

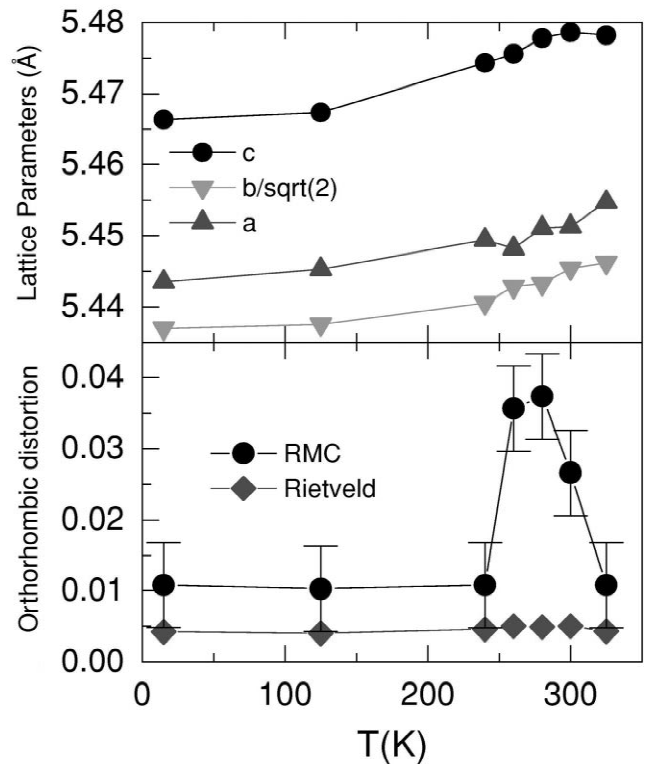


Fig. 3. Behaviour of the fitted lattice constants from the Rietveld refinements (error bars are within the symbols) and of the orthorhombic distortion, defined as $[2\text{MnO}(2) - \text{MnO}(1)]/[\text{MnO}(2) + \text{MnO}(1)]$ calculated from the RMC simulation, versus temperature.

the overlap between both electronic clouds and, therefore, the less efficient the double exchange interaction responsible for the FM coupling observed in these materials.

4. Conclusions

From the RMC analysis of the Bragg and diffuse neutron diffraction intensities the following have been found to be strongly correlated.

A strong distortion in the positions of the Mn atoms in the *ac* plane develops around T_c . As a result, there are Mn atoms whose separation from the NN Mn atom is shorter than that corresponding to the averaged structure. These atoms present smaller Mn–O–Mn angles, shorter Mn–O distances and interact ferromagnetically, with long range interactions at lower temperatures and short range at high temperatures. Within the *ac* plane we also found a significant number of Mn atoms separated from their Mn NN at a distance longer than the average Rietveld distance. These pairs display larger Mn–O–Mn angles, longer Mn–O distances and interact ferromagnetically at lower temperatures, but antiferromagnetically at temperatures around T_c .

The picture emerging from our RMC analysis is fully consistent with the most recent developments in the theory of phase transitions in double exchange materials [6]. These theories postulate that double exchange materials with lower T_c present significant AFM couplings, inhomogeneities near T_c , first-order magnetic transitions and are not metallic in the paramagnetic regime. This would certainly be the case for $\text{La}_{0.67}\text{Ca}_{0.33}\text{MnO}_3$. Within this framework we can also explain the observed differences with the Sr compound, $\text{La}_{0.67}\text{Sr}_{0.33}\text{MnO}_3$. It displays a

higher T_c , goes through a continuous second-order transition and remains metallic in the paramagnetic regime. According to the current predictions [6], double exchange systems showing the above phenomenology should not present an AFM interaction, as is indeed the case [11].

Acknowledgements

The authors are indebted to M.J. Martínez, T. Casais and J.A. Alonso for synthesis of the powder samples and to F. Guinea for helpful conversations. This work was supported by grants CAM 07N/0027/1999 and MAT99/1045.

References

- [1] J.M. Coey, M. Viret, S. Von Molnar, *Adv. Phys.* 48 (1999) 167.
- [2] J. Mira, J. Rivas, F. Rivadulla, C. Vazquez-Vazquez, M.A. Lopez-Quintela, *Phys. Rev. B* 60 (1999) 1.
- [3] C. Zenner, *Phys. Rev. B* 81 (1951) 440.
- [4] C. Zenner, *Phys. Rev. B* 82 (1951) 403.
- [5] A. de Andres, M. García-Hernández, J.L. Martínez, *Phys. Rev. B* 60 (1999) 7328.
- [6] J.L. Alonso, L.A. Fernández, F. Guinea, V. Laliena, V. Matin-Mayor, COND-MAT/0003472.
- [7] J.A. Alonso, M.T. Casais, *Eur. J. Solid State Inorg. Chem.* 33 (1996) 331.
- [8] J.W. Lynn et al., *Phys. Rev. Lett.* 76 (1996) 4046.
- [9] A. Møllergaard, R.L. McGreevy, *Acta Crystallogr. A* 55 (1999) 783.
- [10] S.J.L. Billinge et al., *Phys. Rev. Lett.* 77 (1996) 715.
- [11] A. Møllergaard, R.L. McGreevy, S.G. Eriksson, *J. Phys. Condens. Matter* 12 (2000) 4975.